Supplementary Information

Identification of interaction, surface species and anticorrosion potency for adsorption of myrrh extract on 330 stainless steel in 1 M HCl solution

Arafat Toghan[1*], M. Fakeeh[2], Ahmed Fawzy[3], Hend S. Gadow[2*]

[1]*Chemistry Department, College of Science, Imam Mohammad Ibn Saud Islamic University (IMSIU), Riyadh 11623, Saudi Arabia*

[2]*Higher Institute for Engineering and Technology, New Damietta 42519, Egypt*

[3]*Chemistry Department, Faculty of Science, Assiut University, Assiut 71516, Egypt*

*Corresponding authors: A. Toghan: aatahmed@imamu.edu.sa; H.S. Gadow: hendgadow@gmail.com

Weight loss measurements

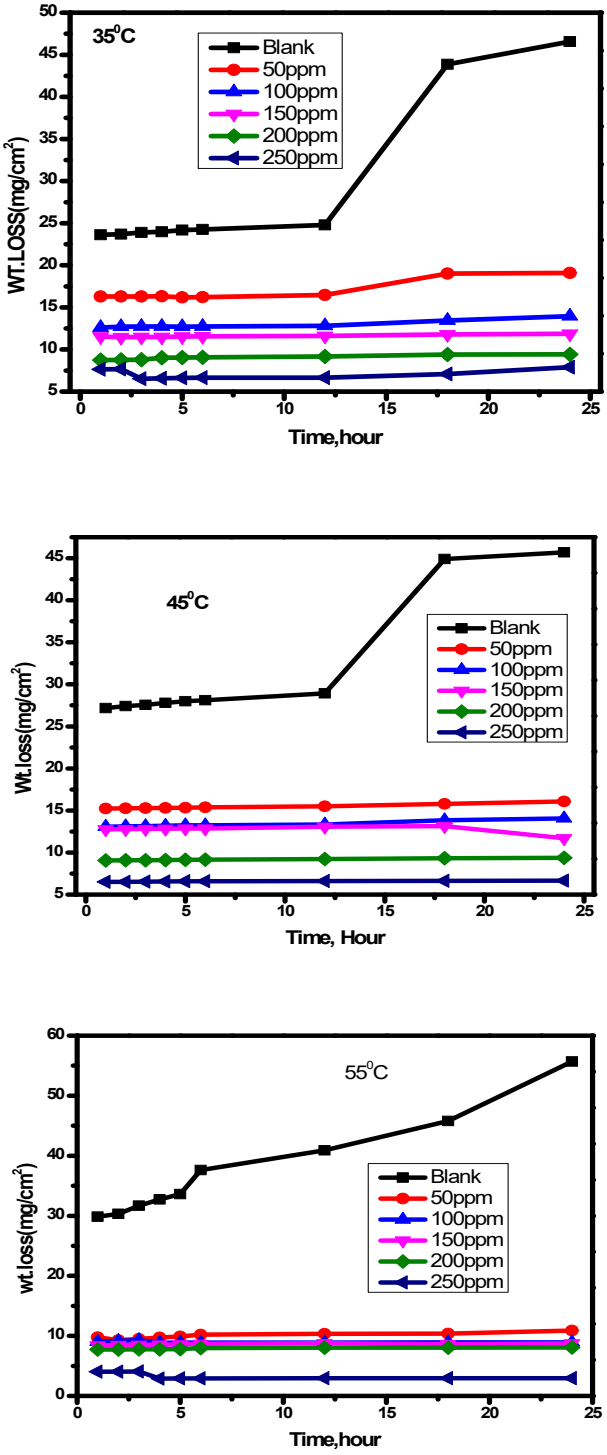

Fig. S1. Weight loss versus immersion time plots for SS samples in 1.0 M HCl solution (blank) and in the presence of various concentrations of myrrh extract at different temperatures.

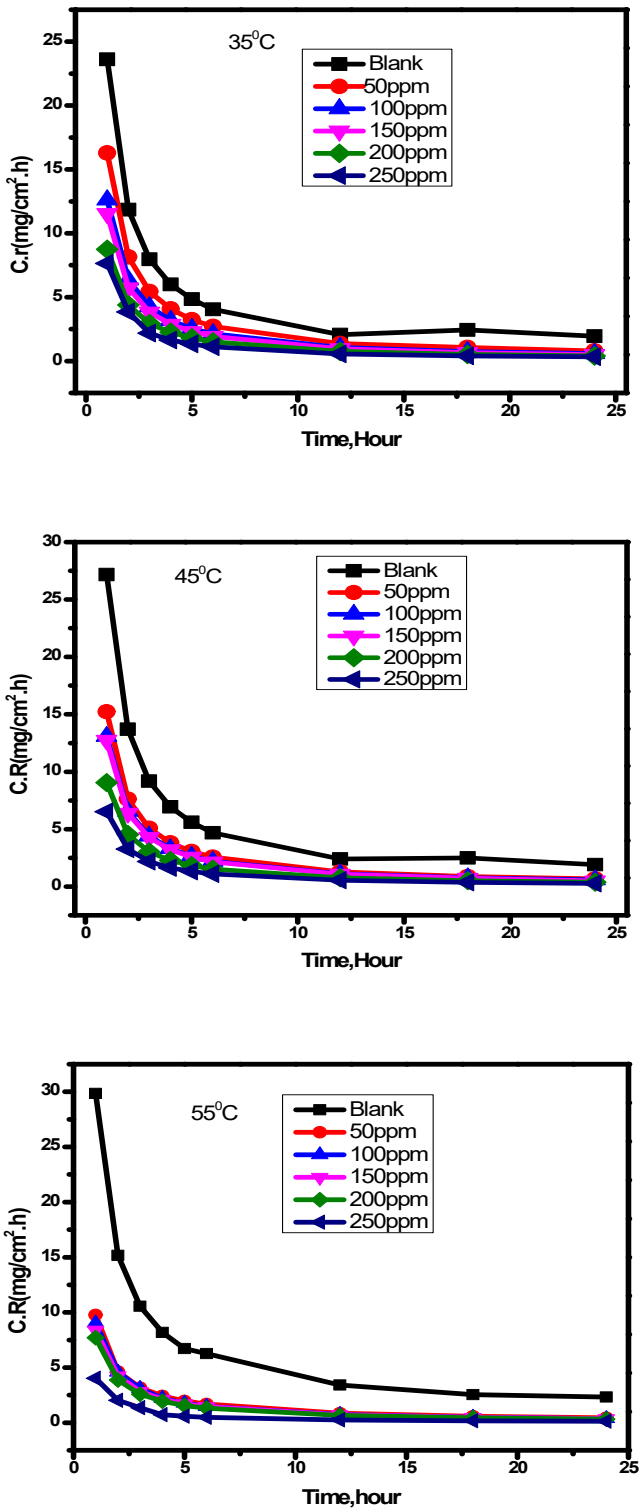

Fig. S2. Variation of corrosion rates of SS in 1.0 M HCl solution with immersion time (1- 24h) in the absence and presence of various concentrations (50-250 ppm) of myrrh extract at different temperatures.

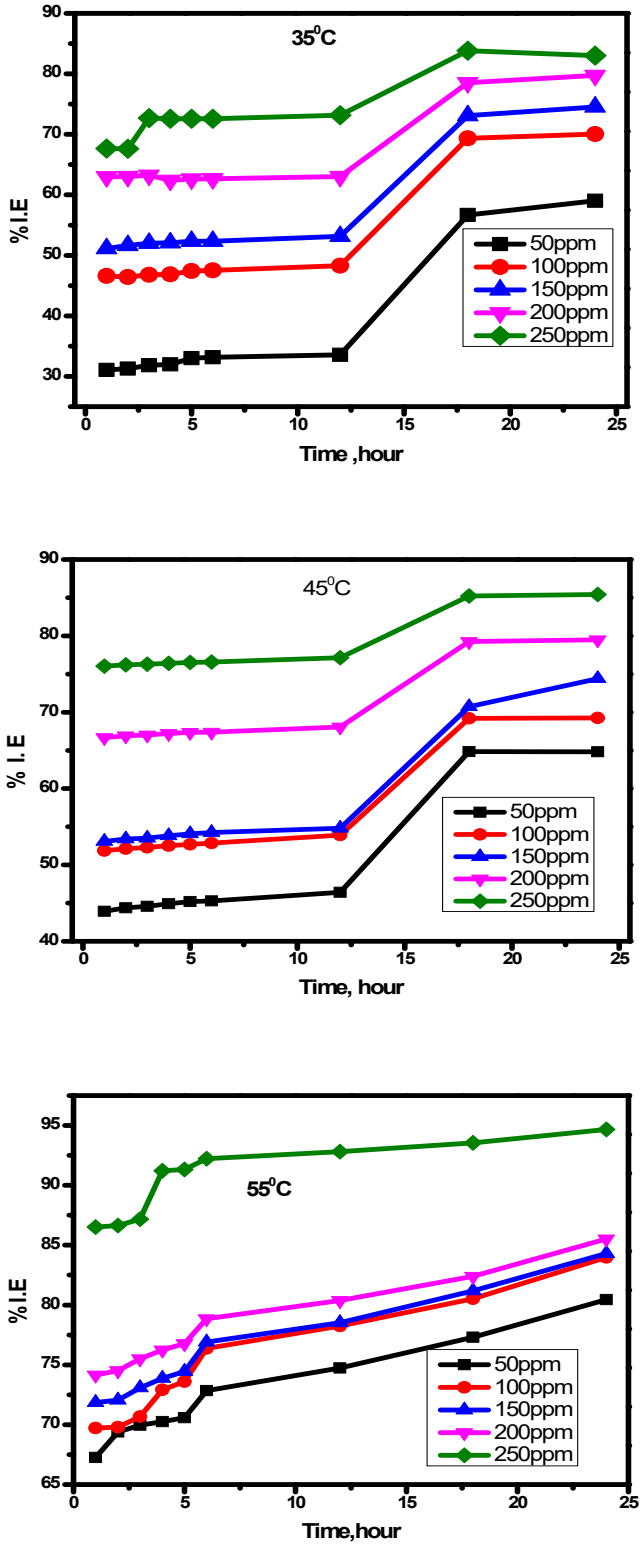

Fig. S3. Variation of inhibition efficiencies (%IE) of various concentrations (50-250 ppm) of myrrh extract with immersion time (1- 24h) in 1.0 M HCl solution at different temperatures.

Adsorption isotherms

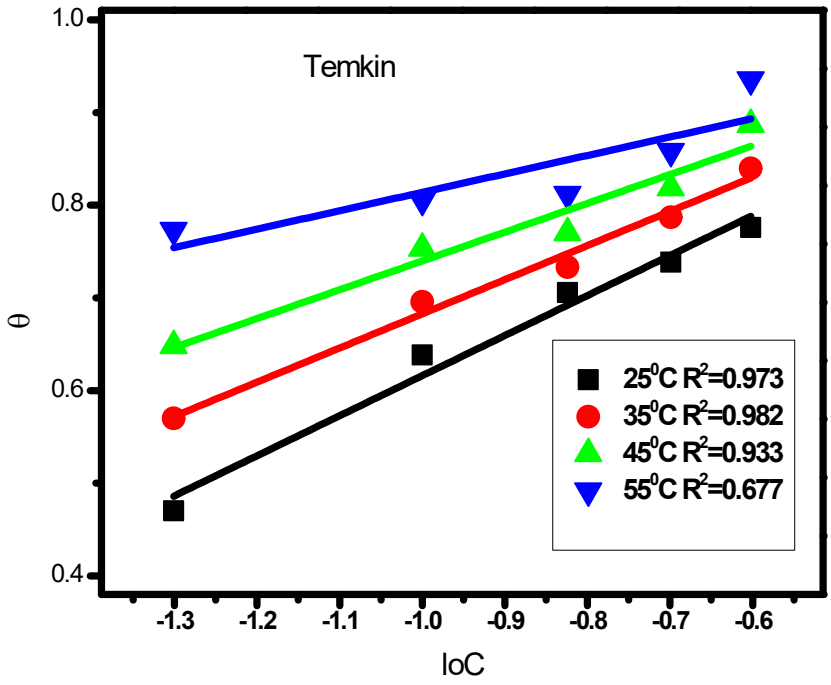

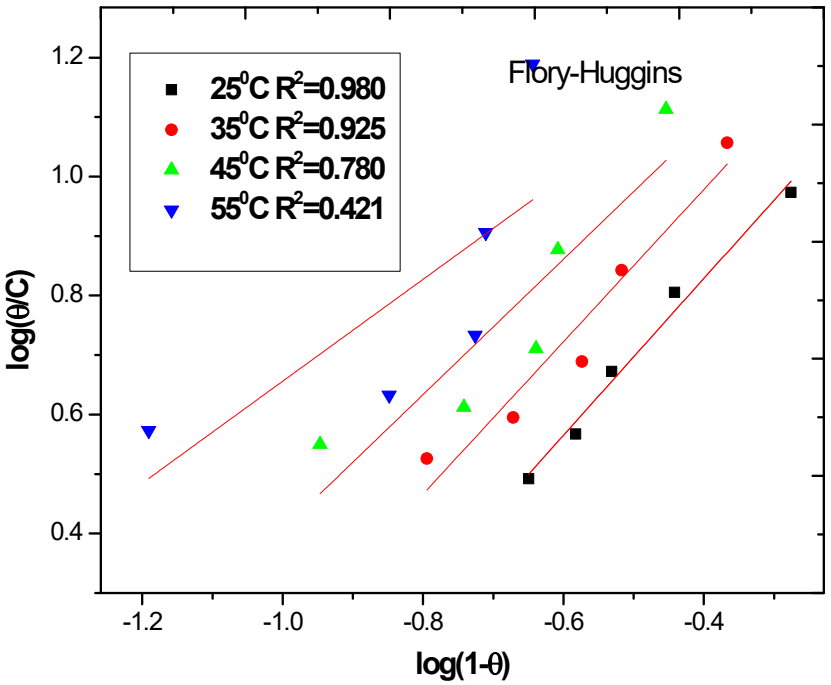

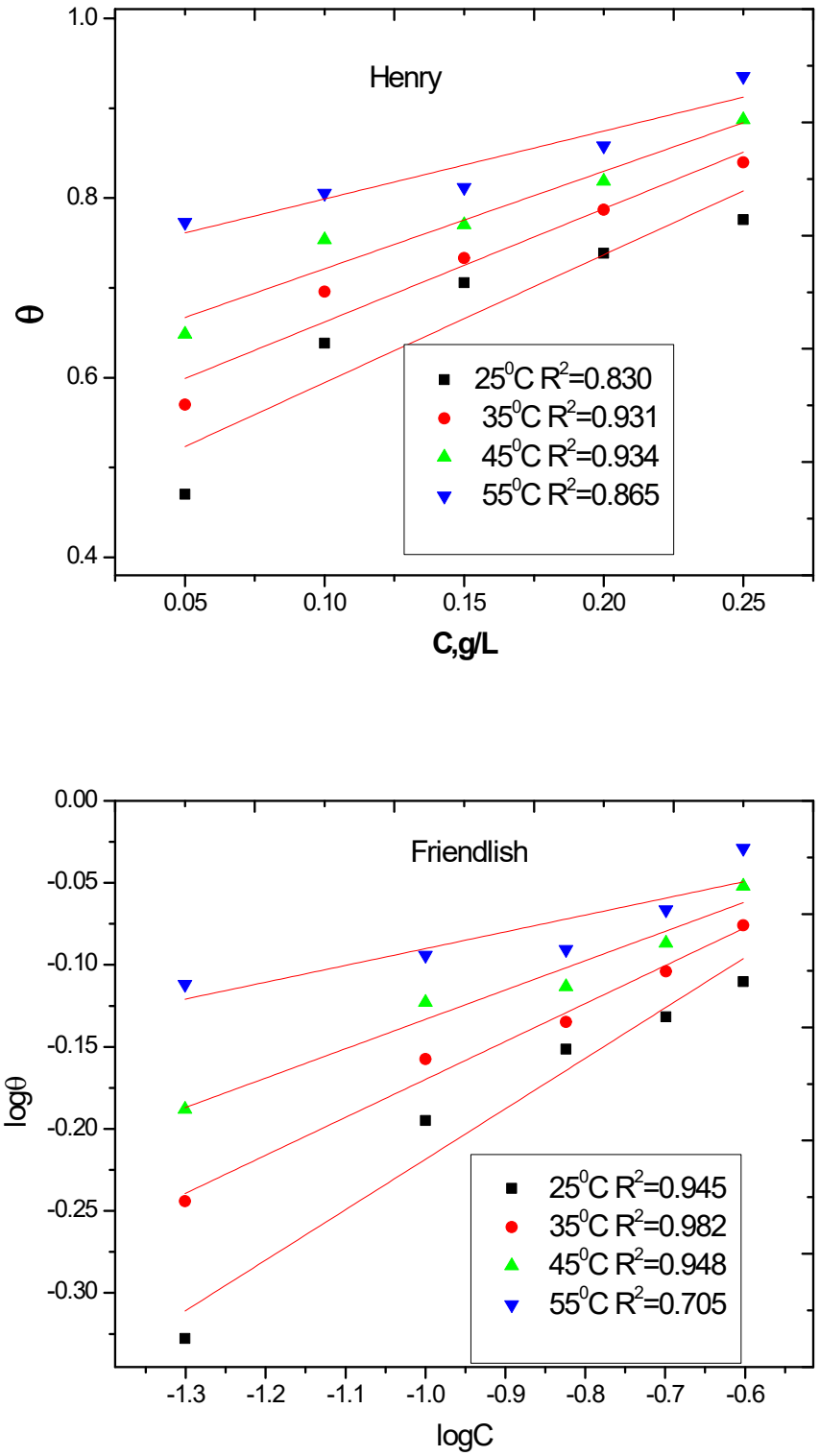

Fig. S4. Temkin, Flory-Huggins, Henry and Freundlich isotherms of the myrrh extract adsorbed on the SS surface during its corrosion in 1.0 M HCl solution at different temperatures (25-55 ^{0}C).

Computational techniques

Density functional theory (DFT) calculations

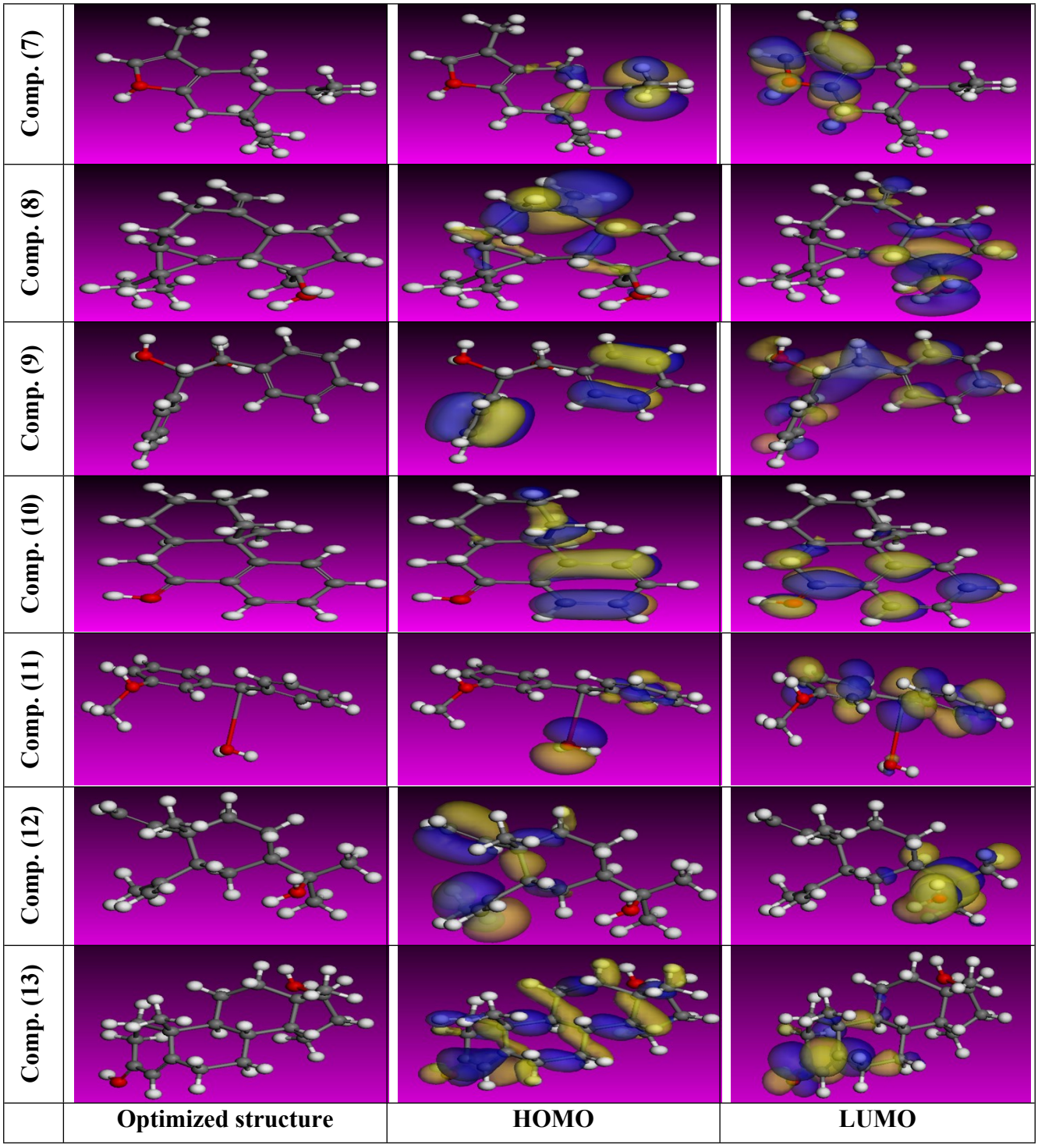

Fig. S5. Optimized molecular structures, LUMO and HOMO for the protonated myrrh extract molecules.

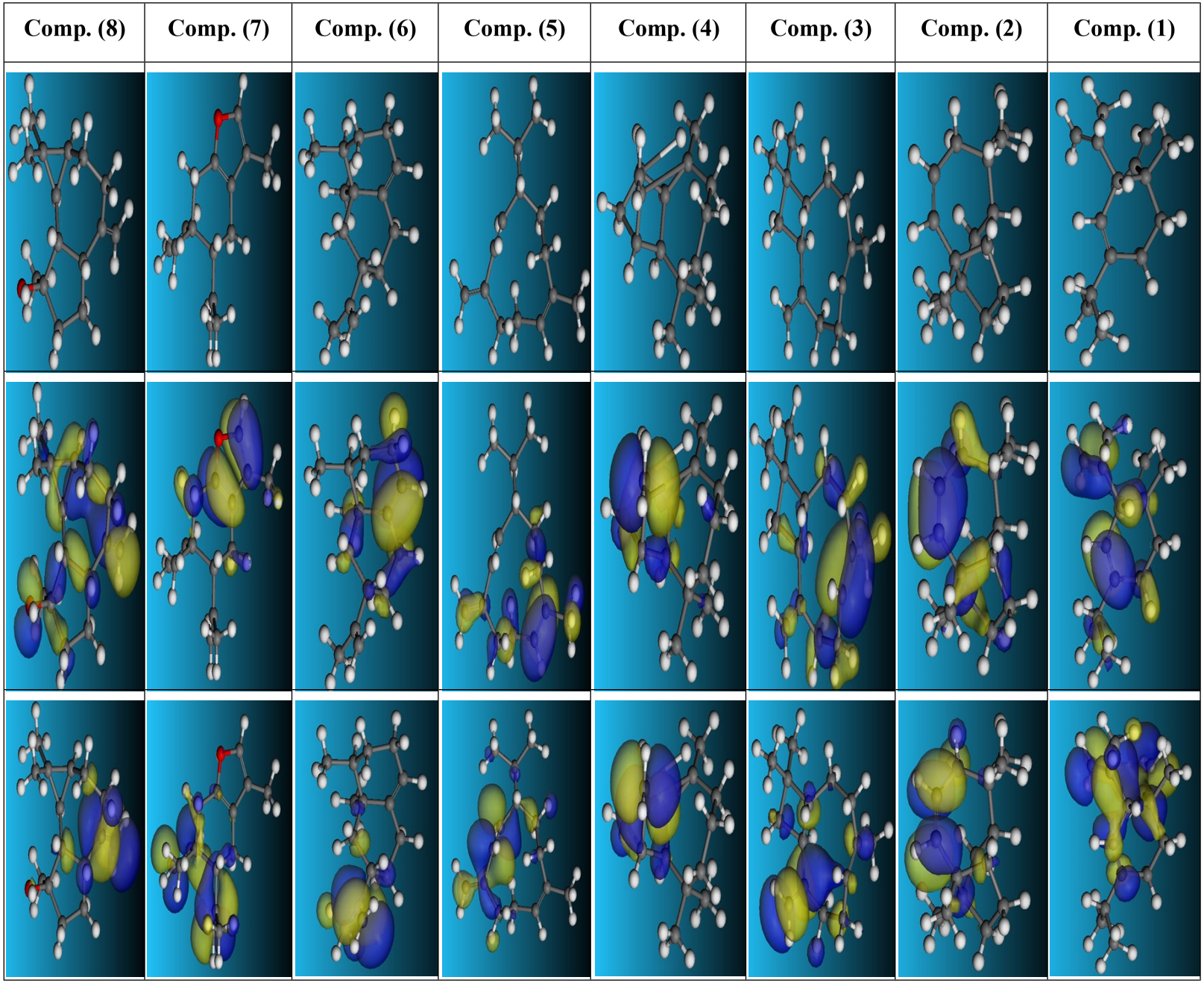
Comp. (8)
Comp. (7)
Comp. (6)
Comp. (5)
Comp. (4)
Comp. (3)
Comp. (2)
Comp. (1)

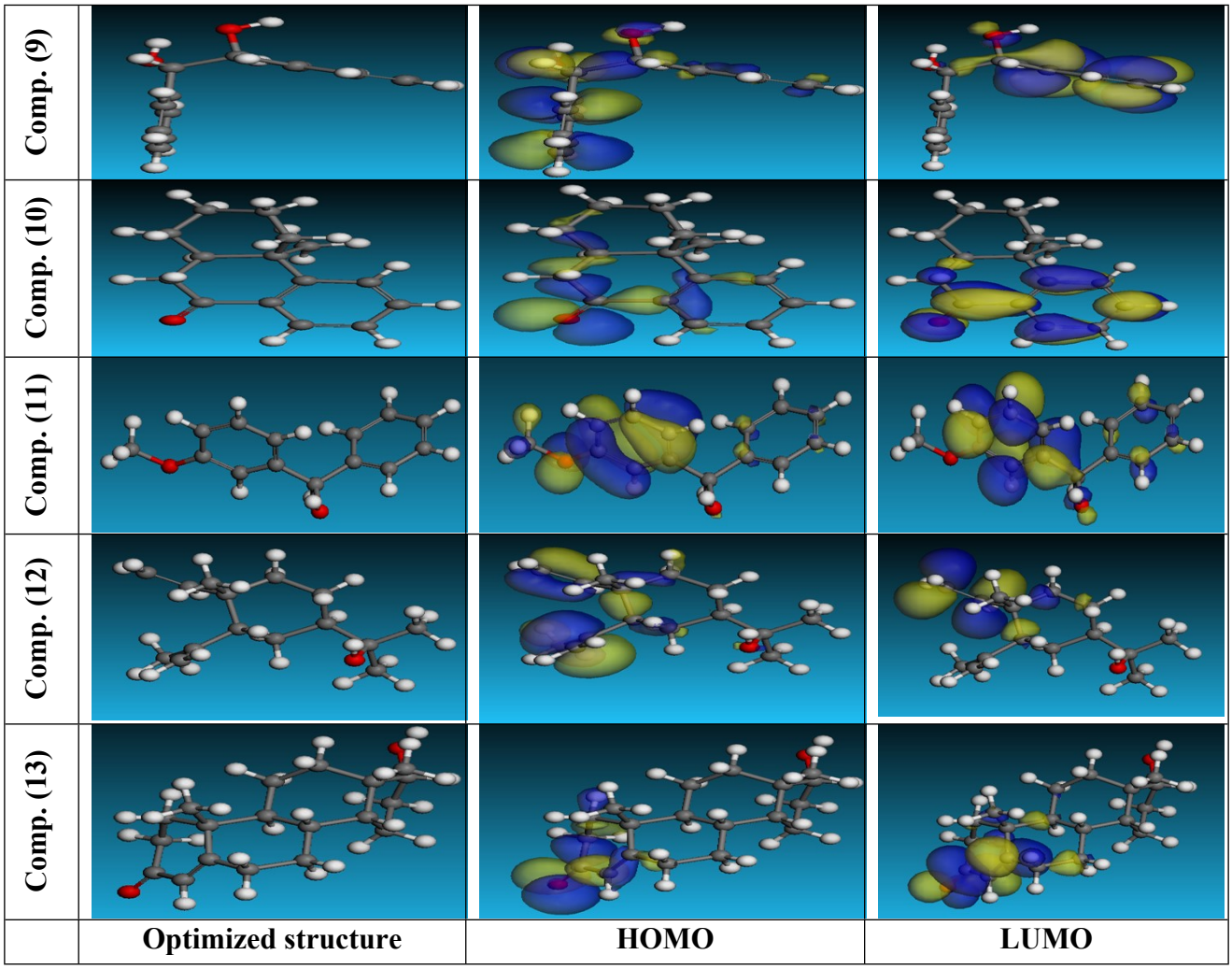

Fig. S6. Optimized molecular structures, LUMO and HOMO for the vacuum myrrh extract molecules.

Table S1. Theoretical parameters of the protonated myrrh extract molecules computed using DFT methods.

Protonated	Comp. (7)	Comp. (8)	Comp. (9)	Comp. (10)
$-E_{HOMO}$ (eV)	-5.624	-5.648	-6.528	-6.334
$-E_{LUMO}$ (eV)	-1.724	-1.193	-3.115	-3.670
ΔE (eV)	3.900	4.460	3.413	2.664
η (eV)	1.950	2.230	1.710	1.330
σ $(eV)^{-1}$	0.512	0.448	0.585	0.752
Pi (e.V)	-7.350	-6.841	-9.643	-10.00
χ (eV)	7.350	6.841	9.643	10.00
Dipole moment	12.783	10.26	14.011	7.411

Molecular area (A°²)	255.66	250.20	247.15	236.73
ω (Electrophilicity index)	13.850	10.49	27.18	37.590
ω^+ (Electro-accepting power)	0.991	1.194	4.614	7.060
ω^- (Electro-donating)	5.541	5.640	4..849	12.060
ε (Nucleophilicity index)	0.072	0.095	0.036	0.026
ΔE Back donation	-0.488	-0.558	-0.428	-0.333
ΔN_{max} (e)	-0.787	-0.574	-1.568	-2.150
Protonated	**Comp. (11)**	**Comp. (12)**	**Comp. (13)**	
$-E_{HOMO}$ (eV)	-6.811	-5.505	-6.765	
$-E_{LUMO}$ (eV)	-4.698	-1.540	-3.606	
ΔE (eV)	2.110	3.970	3.160	
η (eV)	1.060	1.985	1.580	
σ $(eV)^{-1}$	0.943	0.504	0.633	
Pi (e.V)	-11.509	-7.045	-10.371	
χ (eV)	11.509	7.045	10.371	
Dipole moment	8.7555	11.490	11.60	
Molecular area (A°²)	266.14	262.96\	291.48	
ω (Electrophilicity index)	62.480	12.500	34.030	
ω^+ (Electro-accepting power)	12.930	1.616	6.120	
ω^- (Electro-donating)	18.680	5.138	11.300	
ε (Nucleophilicity index)	0.016	0.080	0.029	
ΔE Back donation	-0.206	-0.497	-0.395	
ΔN_{max} (e)	-3.410	-0.696	1.927	

Table S2. Theoretical parameters of the vacuum myrrh extract molecules computed using DFT methods.

Vacuum	**Comp. (1)**	**Comp. (2)**	**Comp. (3)**	**Comp. (4)**	**Comp. (5)**
$-E_{HOMO}$ (eV)	-4.536	-4.523	-4.463	-4.737	-4.574
$-E_{LUMO}$ (eV)	0.338	0.661	0.347	0.800	0.283
ΔE (eV)	4.200	3.860	4.120	3.940	4.291
η (eV)	2.100	1.930	2.060	1.970	2.146
σ $(eV)^{-1}$	0.476	0.518	0.485	0.507	0.466
Pi (e.V)	-4.198	-3.862	-4.120	-3.663	-4.291
χ (eV)	4.198	3.862	4.120	3.660	4.291
Dipole moment	0.701	0.242	0.630	0.450	0.781
ω (Electrophilicity index)	4.190	3.550	4.120	3.405	4.290
ω^+ (Electro-accepting power)	0.459	0.685	0.460	0.809	0.428
ω^- (Electro-donating)	2.896	3.277	2.686	3.577	2.857

ε (Nucleophilicity index)	0.238	0.281	0.243	0.293	0.233
ΔE Back donation	-0.529	-0.483	-0.515	-0.493	-0.537
ΔN_{max} (e)	0.019	0.108	0.039	0.157	0.002
Vacuum	**Comp. (6)**	**Comp. (7)**	**Comp. (8)**	**Comp. (8)**	**Comp. (10)**
$-E_{HOMO}$ (eV)	-4.573	-4.194	-4.684	-5.000	-4.466
$-E_{LUMO}$ (eV)	0.641	0.287	0.639	-0.421	-1.373
ΔE (eV)	3.65	3.90	4.050	4.580	3.090
η (eV)	1.830	1.950	2.030	2.290	1.550
σ $(eV)^{-1}$	0.546	0.512	0.493	0.437	0.645
Pi (e.V)	-3.932	-3.907	-4.045	-5.421	-5.839
χ (eV)	3.932	3.907	4.045	5.421	5.839
Dipole moment	0.466	1.071	1.443	2.4088	3.827
ω (Electrophilicity index)	4.220	4.170	4.030	6.416	10.99
ω^+ (Electro-accepting power)	0.670	0.408	0.673	0.535	1.489
ω^- (Electro-donating)	3.278	2.649	3.330	3.245	4.408
ε (Nucleophilicity index)	0.236	0.239	0.248	0.155	0.091
ΔE Back donation	-0.458	-0.488	-0.508	-0.573	-0.388
ΔN_{max} (e)	0.262	0.096	-0.030	-0.266	-0.503
Vacuum	**Comp. (11)**	**Comp. (12)**	**Comp. (13)**		
$-E_{HOMO}$ (eV)	-4.552	-4.708	-4.215		
$-E_{LUMO}$ (eV)	-0.347	0.544	-1.219		
ΔE (eV)	4.550	4.160	3.000		
η (eV)	2.280	2.080	1.500		
σ $(eV)^{-1}$	0.439	0.480	0.601		
Pi (e.V)	-4.899	-4.164	-5.434		
χ (eV)	4.899	4.164	5.434		
Dipole moment	3.113	1.856	5.904		
ω (Electrophilicity index)	5.263	4.168	9.842		
ω^+ (Electro-accepting power)	0.465	0.603	1.292		
ω^- (Electro-donating)	2.914	3.229	4.000		
ε (Nucleophilicity index)	0.190	0.240	0.102		
ΔE Back donation	-0.570	-0.520	-0.375		
ΔN_{max} (e)	-0.136	0.028	-0.354		

Molecular dynamic (MD) simulation

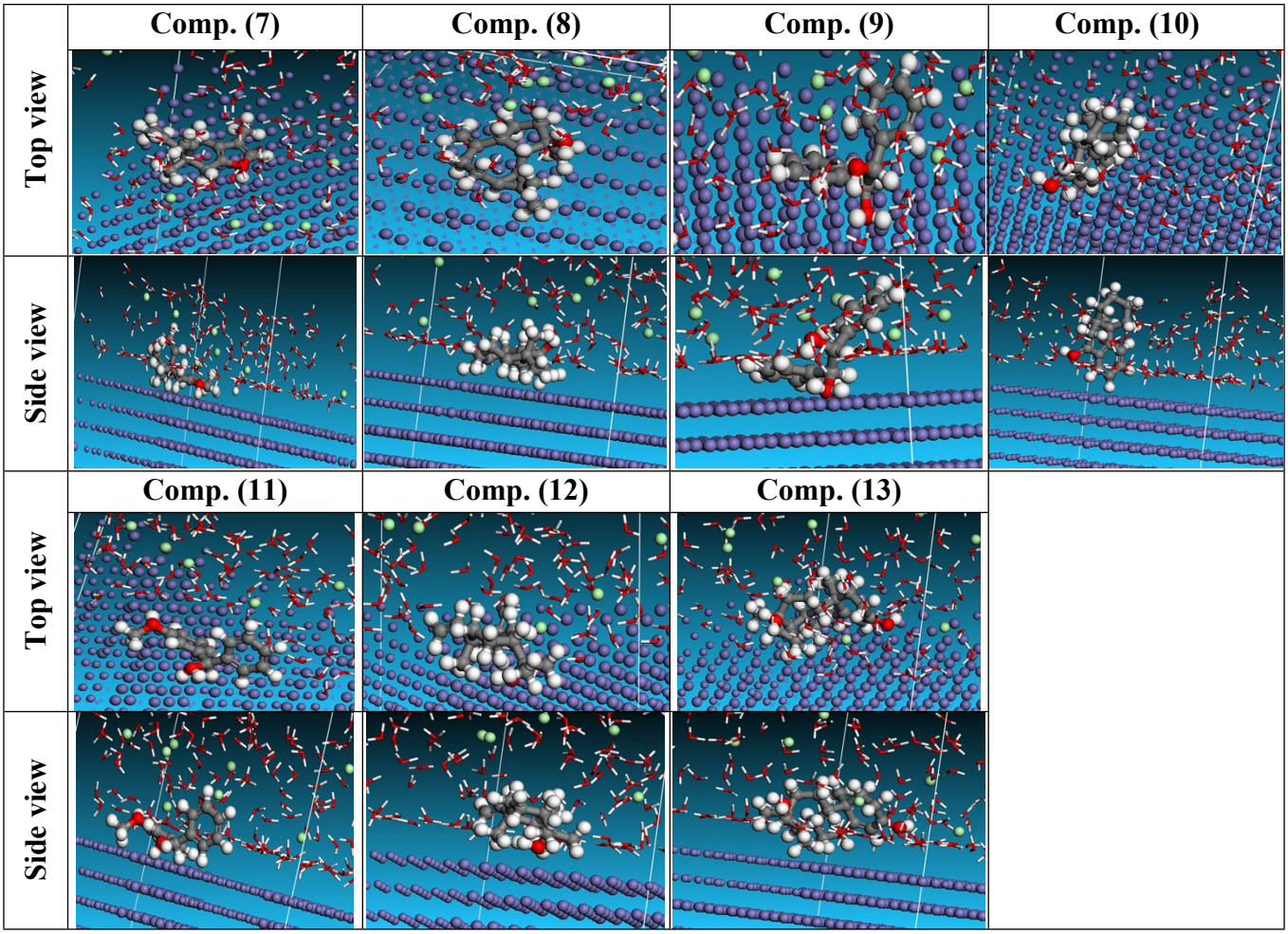

Fig. S7. Top and side views of the most stable adsorption configuration for the protonated myrrh extract molecules computed using MD simulation at the Fe(110) substrate.

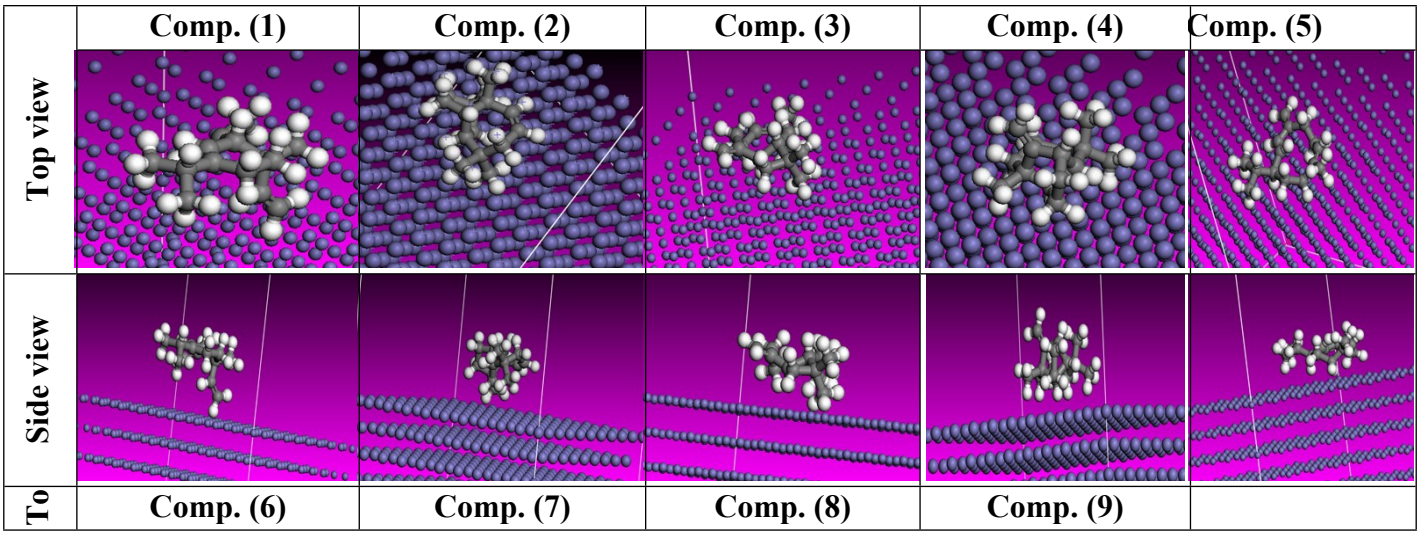

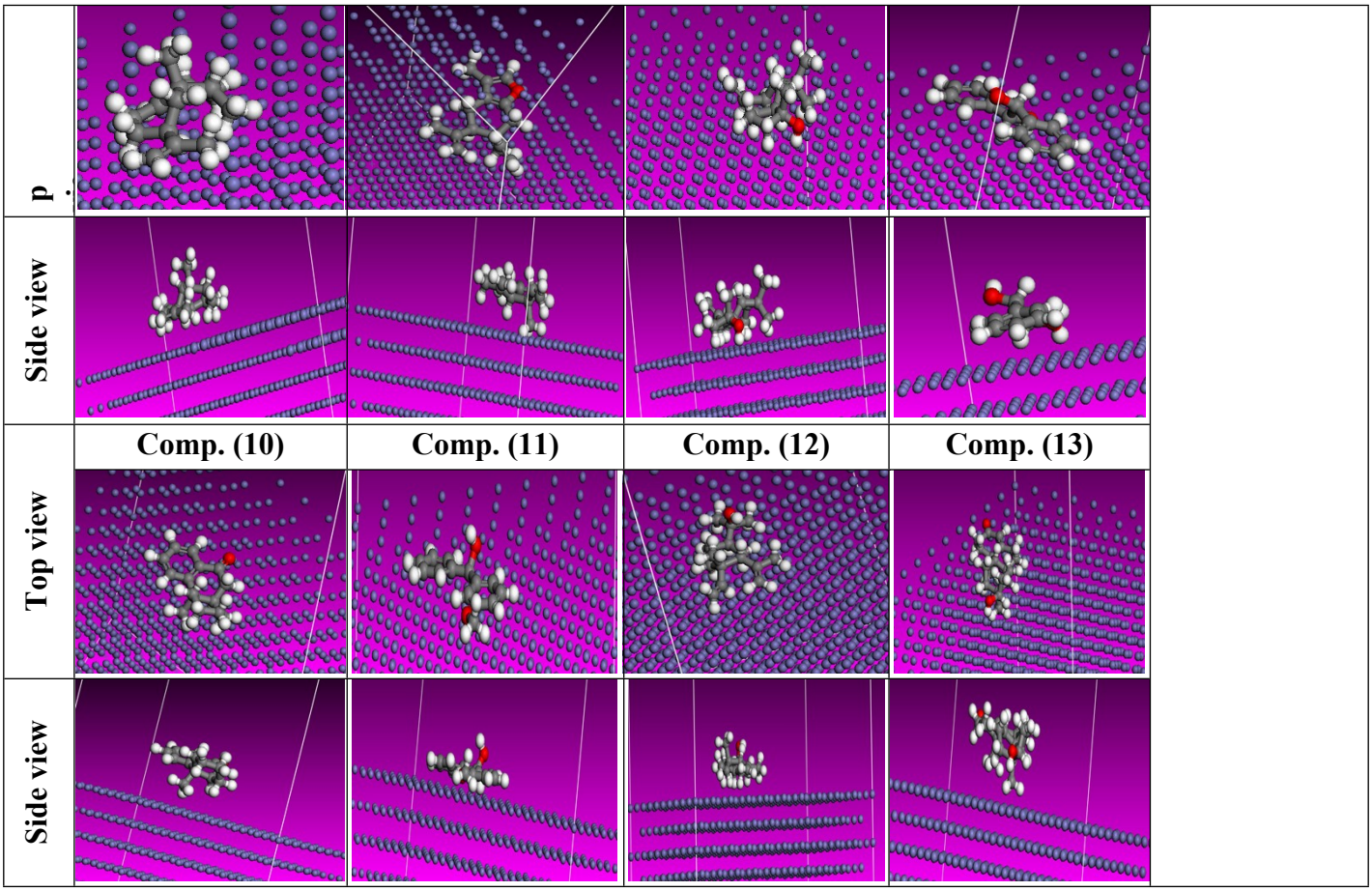

Fig. S8. Top and side views of the most stable adsorption configuration for the vacuum myrrh extract molecules computed using MD simulation at the Fe(110) substrate.

Table S3. Theoretical parameters of protonated myrrh extract molecules computed using MD simulation.

Factors	Comp. (7)	Comp. (8)	Comp. (9)	Comp. (10)
Total energy (kcal mol^{-1})	-6907.746	-6681.620	-6814.845	-6869.643
Adsorption energy (kcal mol^{-1})	-6899.542	-6711.242	-6860.449	-6864.823
Rigid adsorption energy (kcal mol^{-1})	-7100.201	-6910.951	-7053.009	-7057.847
Deformation energy (kcal mol^{-1})	200.660	199.710	192.560	193.020
dE_{ad}/dNi (kcal mol^{-1})	-117.290	-102.750	-51.570	-28.030
dE_{ads} / dNi (kcal mol^{-1}) for water	-13.340	-7.880	-8.770	-13.440
Factors	**Comp. (11)**	**Comp. (12)**	**Comp. (13)**	
Total energy (kcal mol^{-1})	-6697.240	-6751.528	-6738.279	
Adsorption energy (kcal mol^{-1})	-6711.463	-6679.835	-6702.847	
Rigid adsorption energy (kcal mol^{-1})	-6900.007	-6861.019	-6889.316	
Deformation energy (kcal mol^{-1})	188.544	181.180	186.470	
dE_{ad}/dNi (kcal mol^{-1})	-126.270	-98.650	-111.020	
dE_{ads} / dNi (kcal mol^{-1}) for water	-8.740	-7.710	-9.870	

Table S4. Theoretical parameters of vacuum myrrh extract molecules computed using MD simulation.

Factors	Comp. (1)	Comp. (2)	Comp. (3)	Comp. (4)	Comp. (5)
Total energy (kcal mol^{-1})	-128.27	-103.00	-120.96	-107.78	-128.00
Adsorption energy (kcal mol^{-1})	-102.11	-83.31	-103.87	-87.13	-128.45
Rigid adsorption energy (kcal mol^{-1})	-107.61	-84.79	-109.45	-88.85	-120.91
Deformation energy (kcal mol^{-1})	5.490	1.477	5.580	1.720	-7.550
dE_{ad}/dNi (kcal mol^{-1})	-102.11	-83.31	-103.87	-87.13	-128.45
Factors	**Comp. (6)**	**Comp. (7)**	**Comp. (8)**	**Comp. (9)**	
Total energy (kcal mol^{-1})	-130.38	-124.88	-48.26	-77.62	
Adsorption energy (kcal mol^{-1})	-105.92	-108.47	-293.45	-104.00	
Rigid adsorption energy (kcal mol^{-1})	-115.63	-120.99	-99.72	-112.83	
Deformation energy (kcal mol^{-1})	9.710	12.530	-193.72	-112.83	
dE_{ad}/dNi (kcal mol^{-1})	-105.92	-108.47	-293.45	-104.00	
Factors	**Comp. (10)**	**Comp. (11)**	**Comp. (12)**	**Comp. (13)**	
Total energy (kcal mol^{-1})	-120.21	-93.74	-159.41	-191.40	
Adsorption energy (kcal mol^{-1})	-113.72	-113.96	-107.27	-122.41	
Rigid adsorption energy (kcal mol^{-1})	-107.85	-124.75	-117.89	-130.44	
Deformation energy (kcal mol^{-1})	-5.870	10.790	10.620	8.040	
dE_{ad}/dNi (kcal mol^{-1})	-113.72	-113.96	-107.27	-122.41	

Molecular electrostatic potential (MESP)

Protonated

Comp. (7)	Comp. (8)	Comp. (9)	Comp. (10)
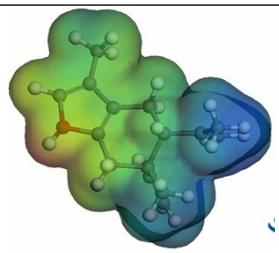	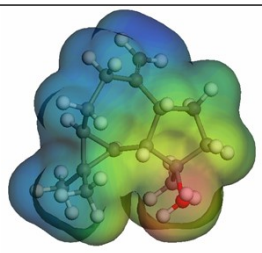	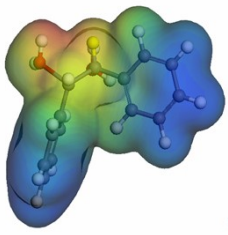	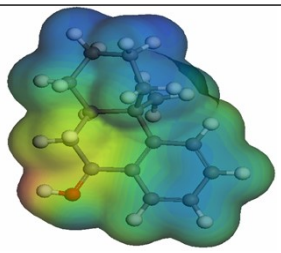
Comp. (11)	**Comp. (12)**	**Comp. (13)**	
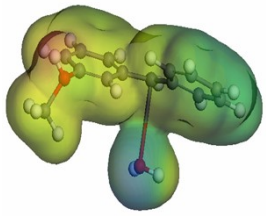	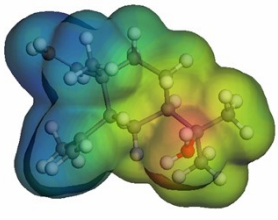	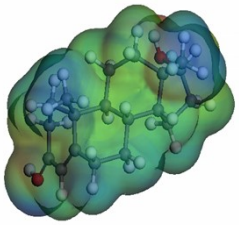	

Fig. S9. Illustrations showing that the hydrogen atoms depicted in blue are particularly vulnerable to nucleophilic attack.

Vacuum

Comp. (1)	Comp. (2)	Comp. (3)	Comp. (4)
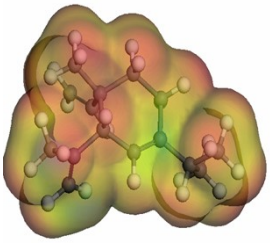	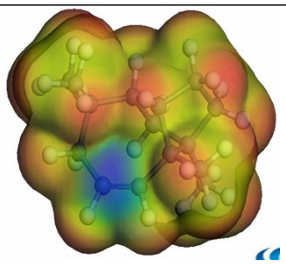	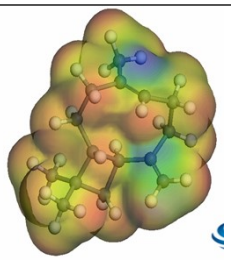	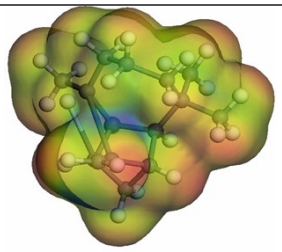
Comp. (5)	**Comp. (6)**	**Comp. (7)**	**Comp. (8)**
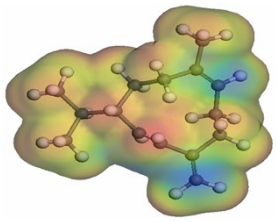	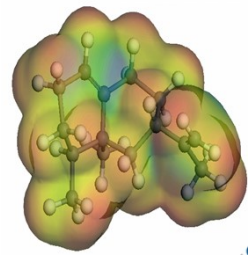	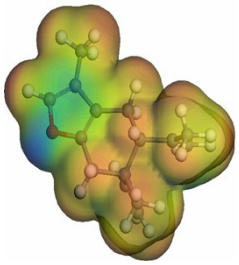	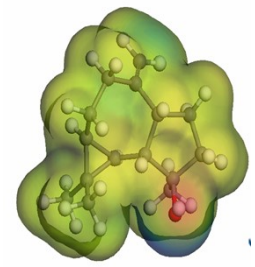
Comp. (9)	**Comp. (10)**	**Comp. (11)**	**Comp. (12)**
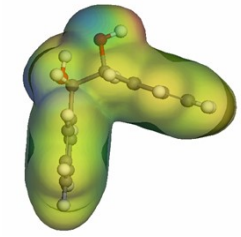	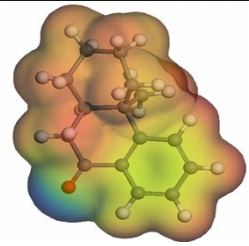	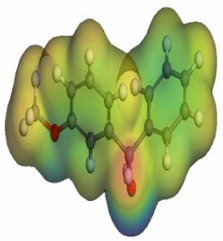	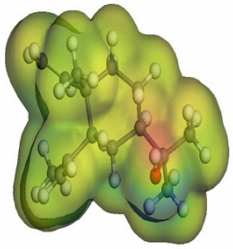
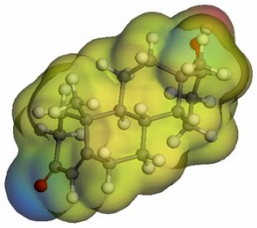 **Comp. (13)**			

Fig. S10. Illustrations showing that the hydrogen atoms depicted in blue are particularly vulnerable to nucleophilic attack.

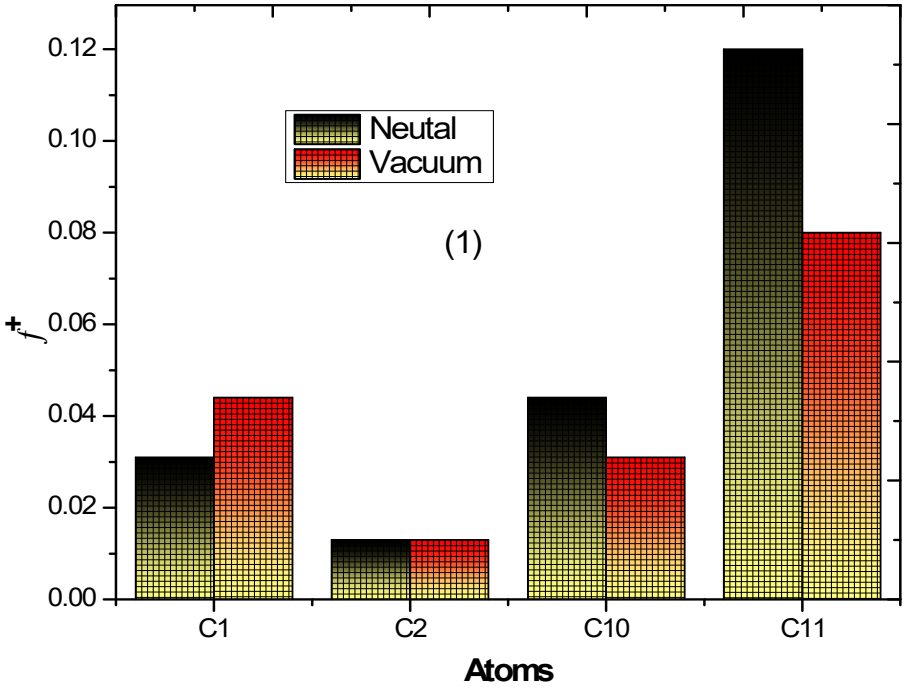
0.12
0.10
0.08
0.06
0.04
0.02
0.00
f^+
Neutal
Vacuum
(1)
C1
C2
C10
C11
Atoms

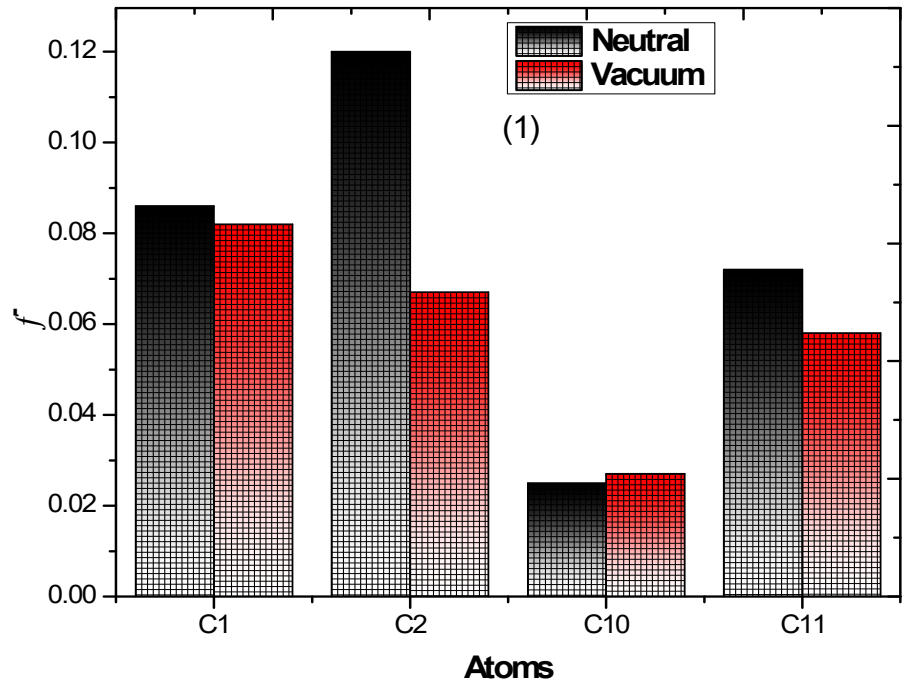
0.12
0.10
0.08
0.06
0.04
0.02
0.00
f^-
Neutral
Vacuum
(1)
C1
C2
C10
C11
Atoms

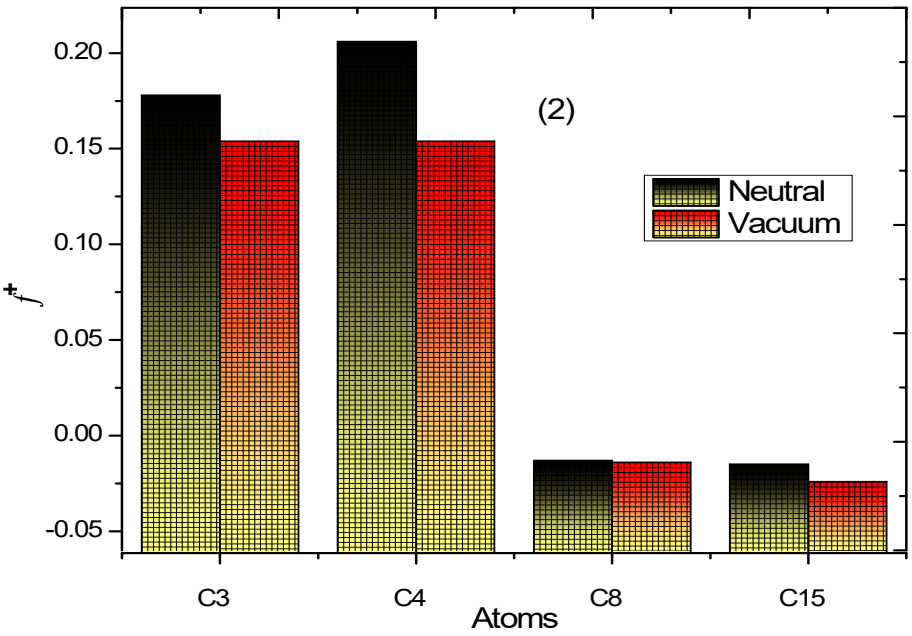
0.20
0.15
0.10
0.05
0.00
-0.05
f^+
(2)
Neutral
Vacuum
C3
C4
C8
C15
Atoms

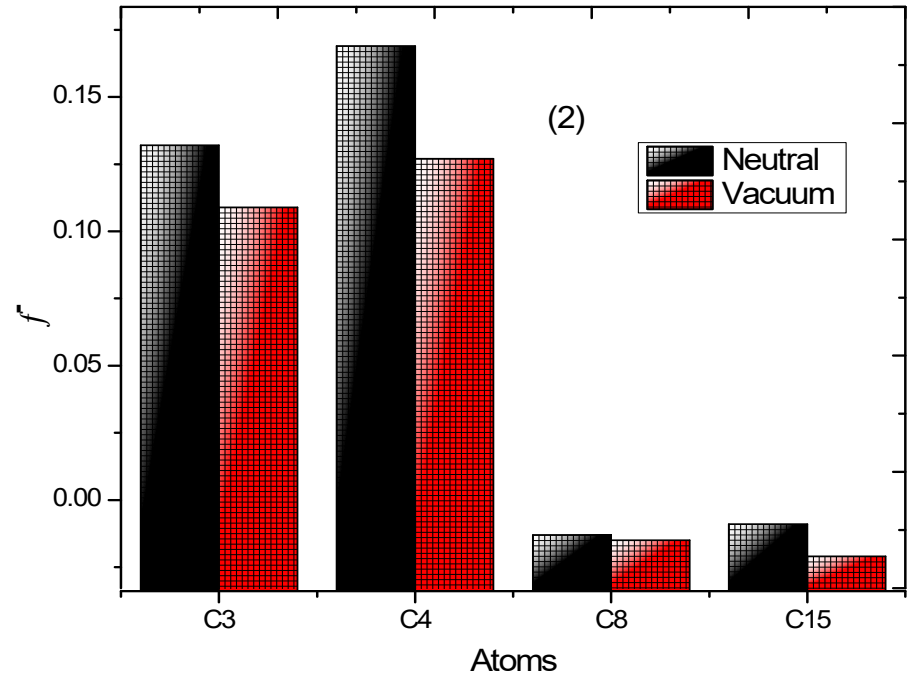
0.15
0.10
0.05
0.00
f^-
(2)
Neutral
Vacuum
C3
C4
C8
C15
Atoms

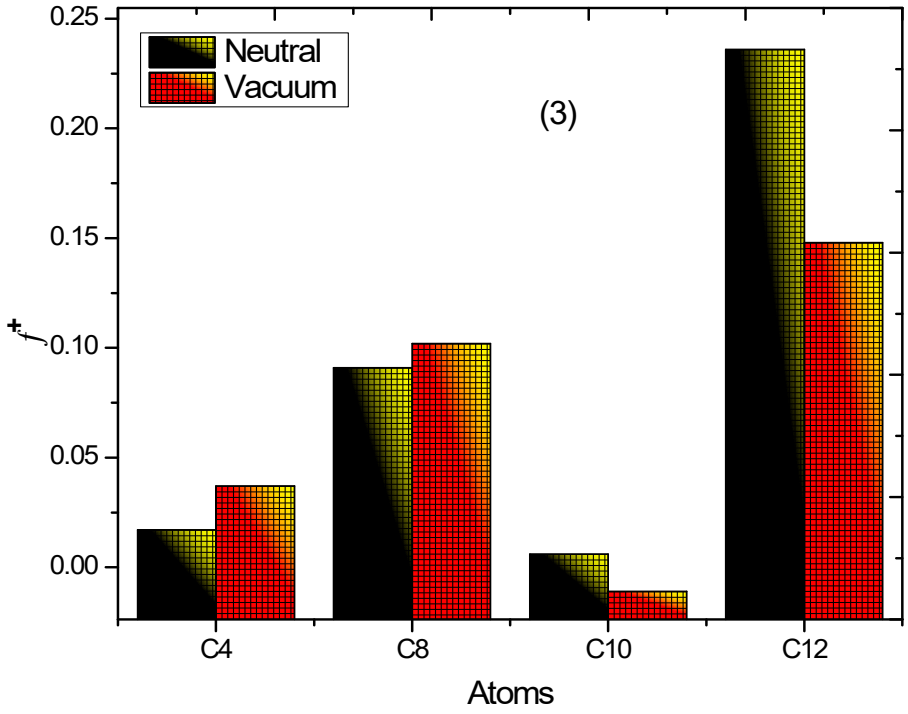
0.25
0.20
0.15
0.10
0.05
0.00
f^+
Neutral
Vacuum
(3)
C4
C8
C10
C12
Atoms

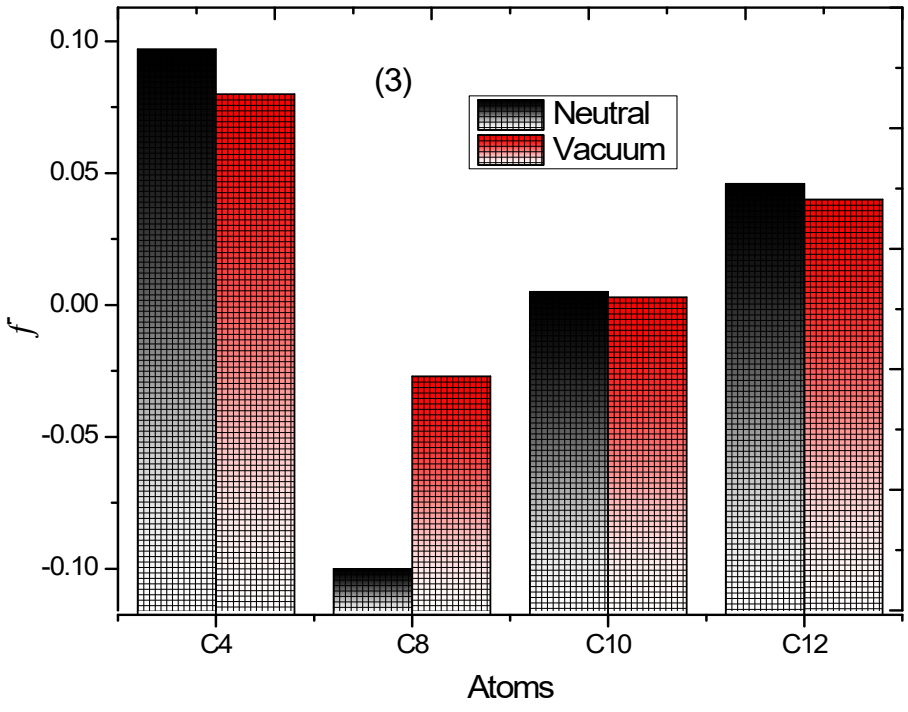
0.10
0.05
0.00
-0.05
-0.10
f^-
(3)
Neutral
Vacuum
C4
C8
C10
C12
Atoms

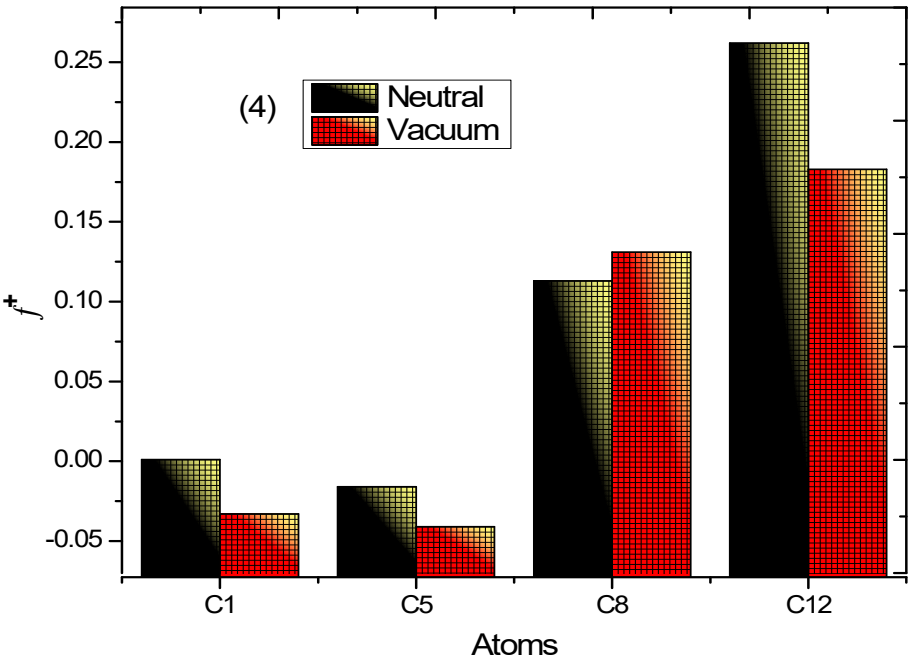
(4)
Neutral
Vacuum
0.25
0.20
0.15
0.10
0.05
0.00
-0.05
f^+
C1
C5
C8
C12
Atoms

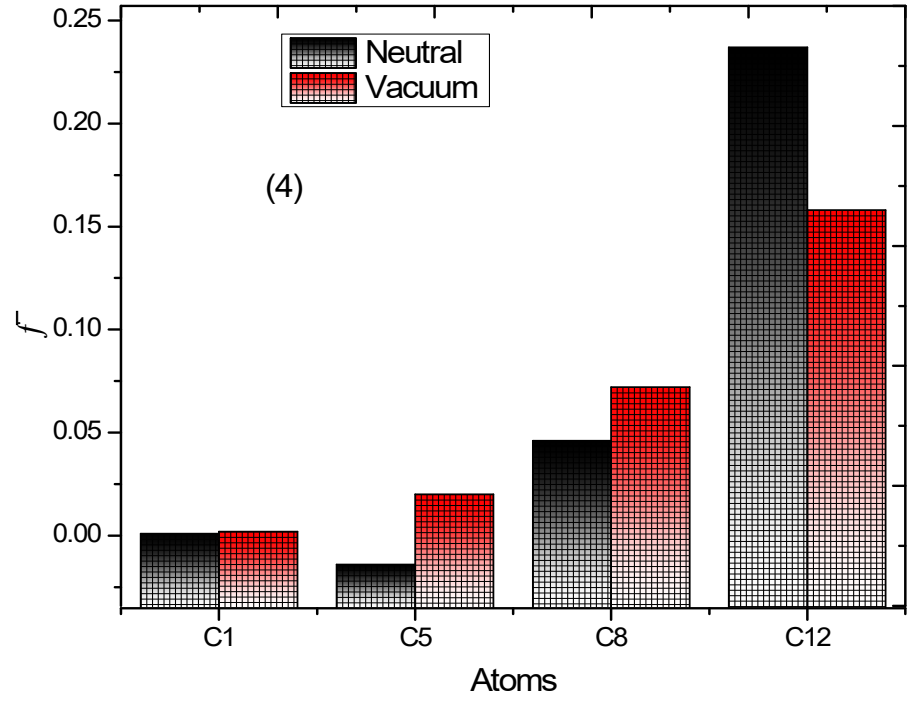
(4)
Neutral
Vacuum
0.25
0.20
0.15
0.10
0.05
0.00
f^-
C1
C5
C8
C12
Atoms

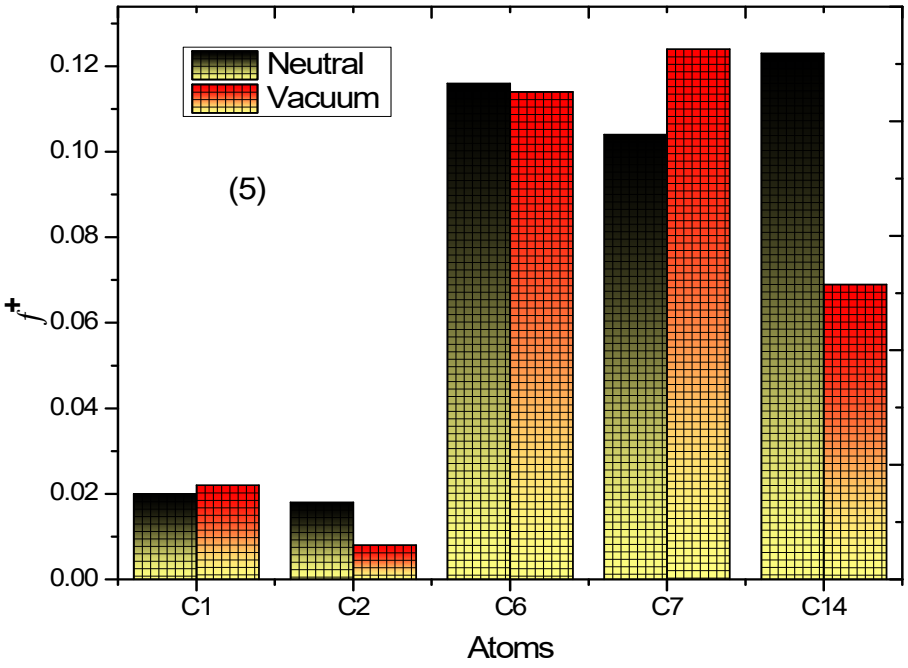
Neutral
Vacuum
(5)
f^+
0.12
0.10
0.08
0.06
0.04
0.02
0.00
C1
C2
C6
C7
C14
Atoms

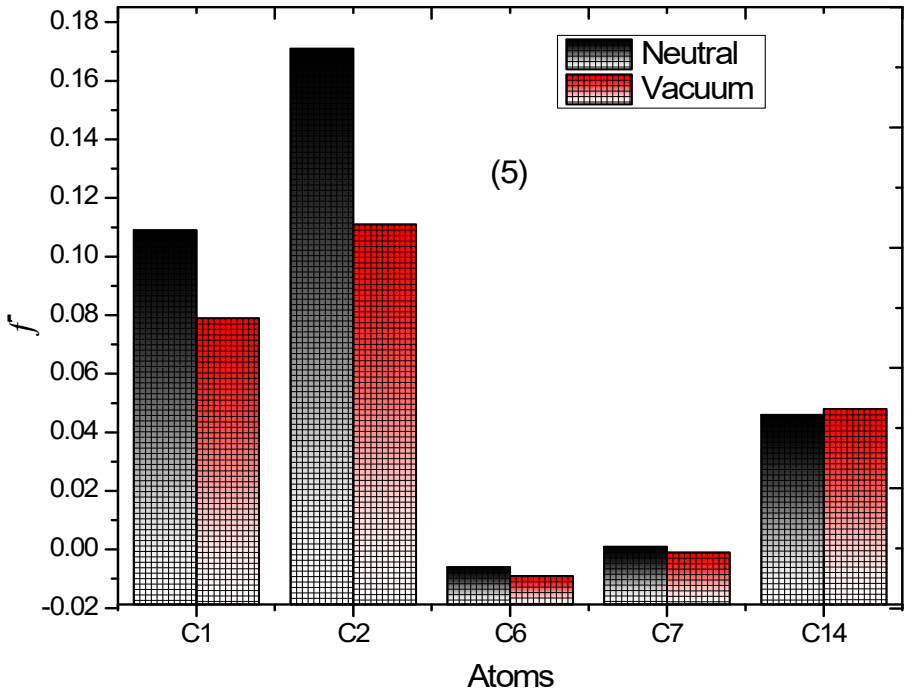
Neutral
Vacuum
(5)
f^-
0.18
0.16
0.14
0.12
0.10
0.08
0.06
0.04
0.02
0.00
-0.02
C1
C2
C6
C7
C14
Atoms

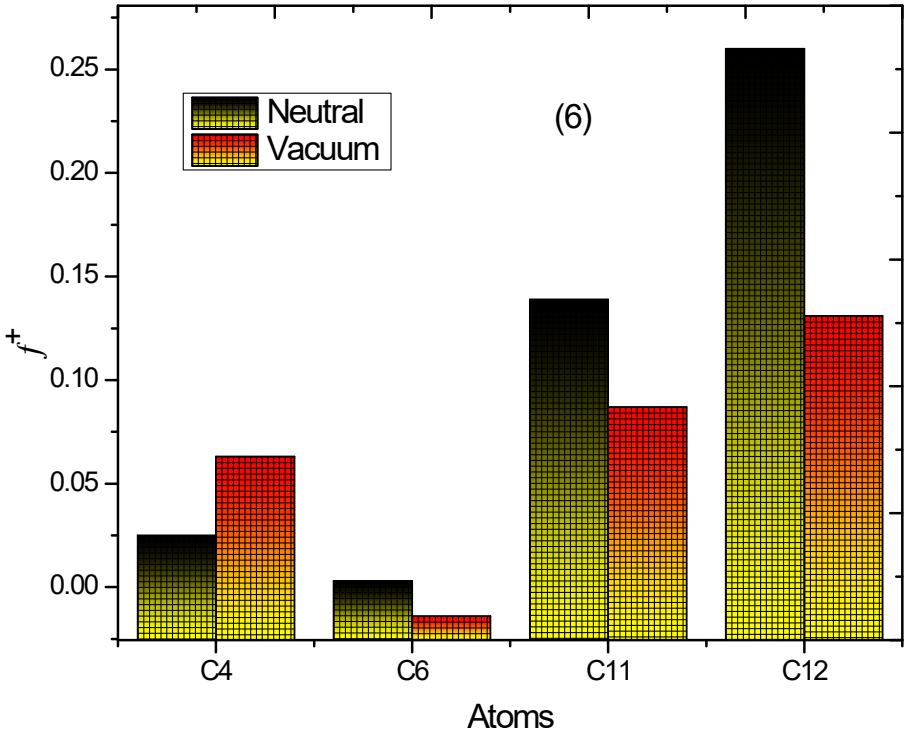
Neutral
Vacuum
(6)
0.25
0.20
0.15
0.10
0.05
0.00
f+
C4
C6
C11
C12
Atoms

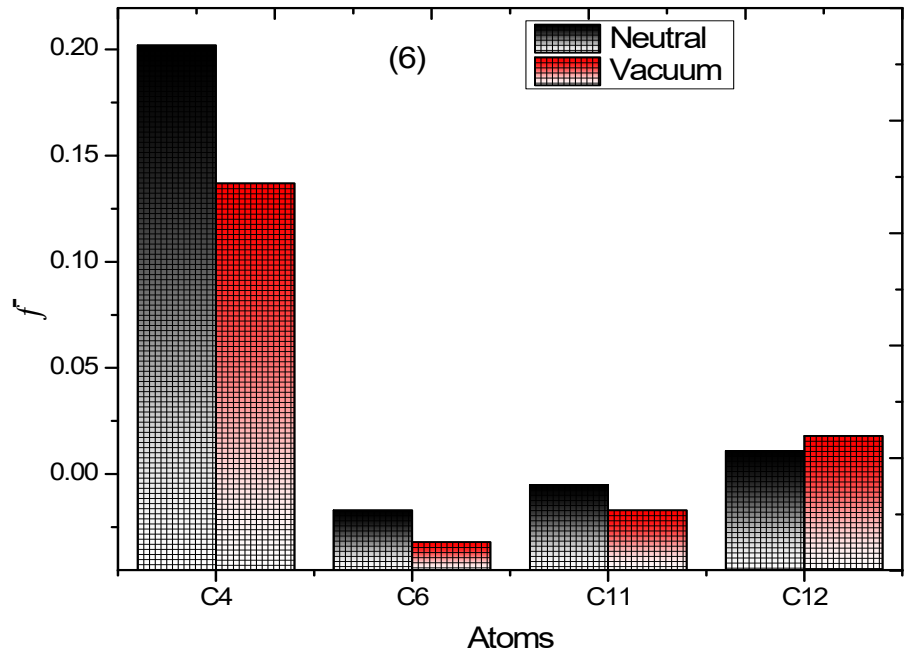
Neutral
Vacuum
(6)
0.20
0.15
0.10
0.05
0.00
f-
C4
C6
C11
C12
Atoms

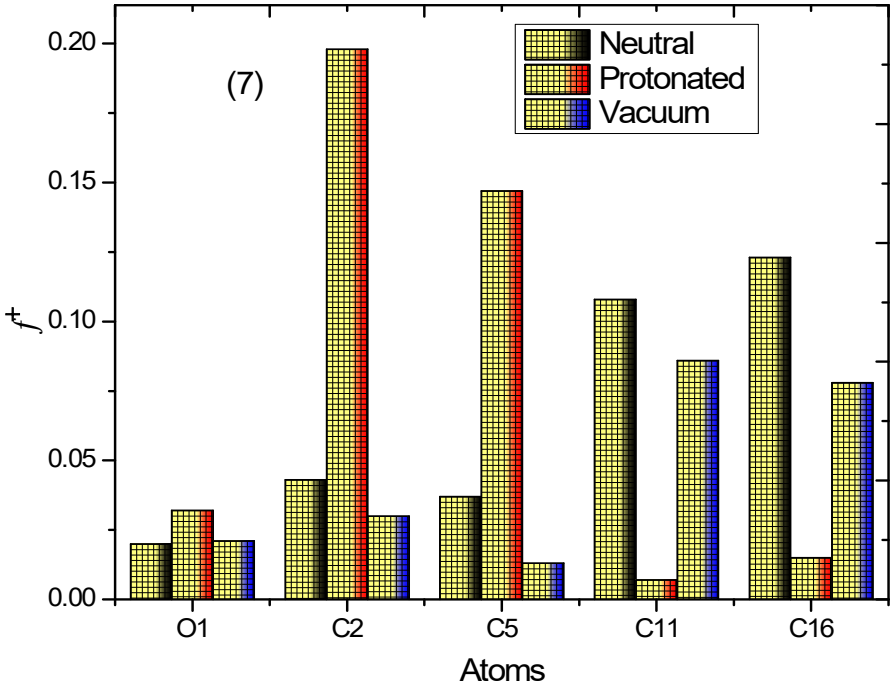
(7)
Neutral
Protonated
Vacuum
0.20
0.15
0.10
0.05
0.00
f^+
O1
C2
C5
C11
C16
Atoms

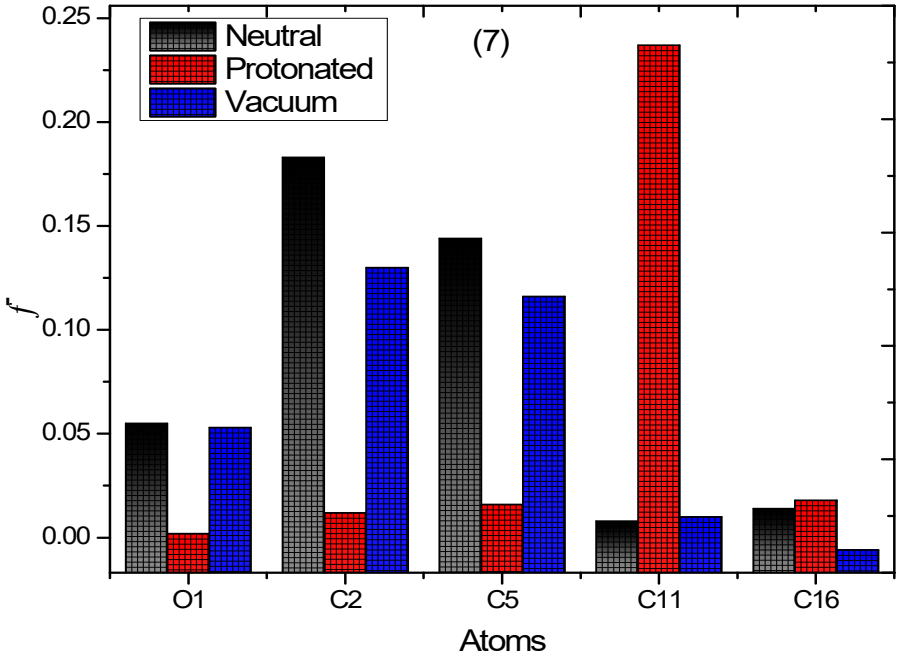
(7)
Neutral
Protonated
Vacuum
0.25
0.20
0.15
0.10
0.05
0.00
f^-
O1
C2
C5
C11
C16
Atoms

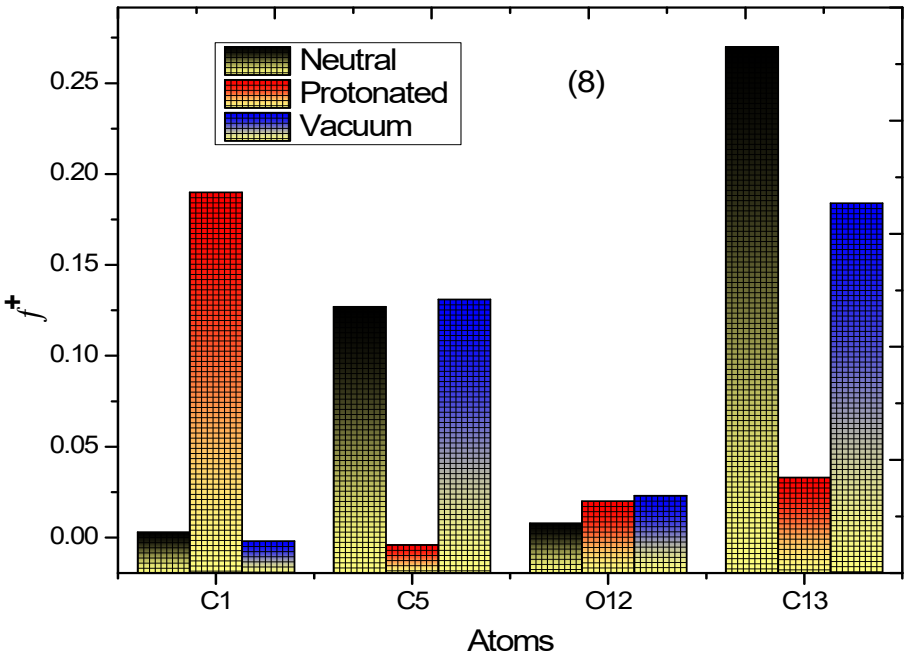
Neutral
Protonated
Vacuum
(8)
0.25
0.20
0.15
0.10
0.05
0.00
f+
C1
C5
O12
C13
Atoms

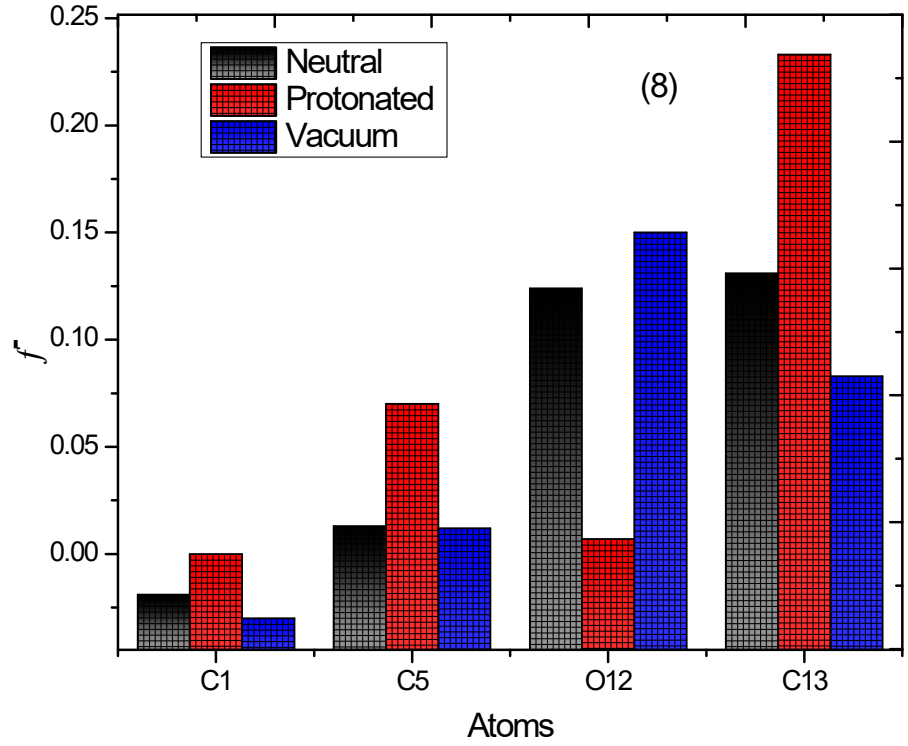
Neutral
Protonated
Vacuum
(8)
0.25
0.20
0.15
0.10
0.05
0.00
f-
C1
C5
O12
C13
Atoms

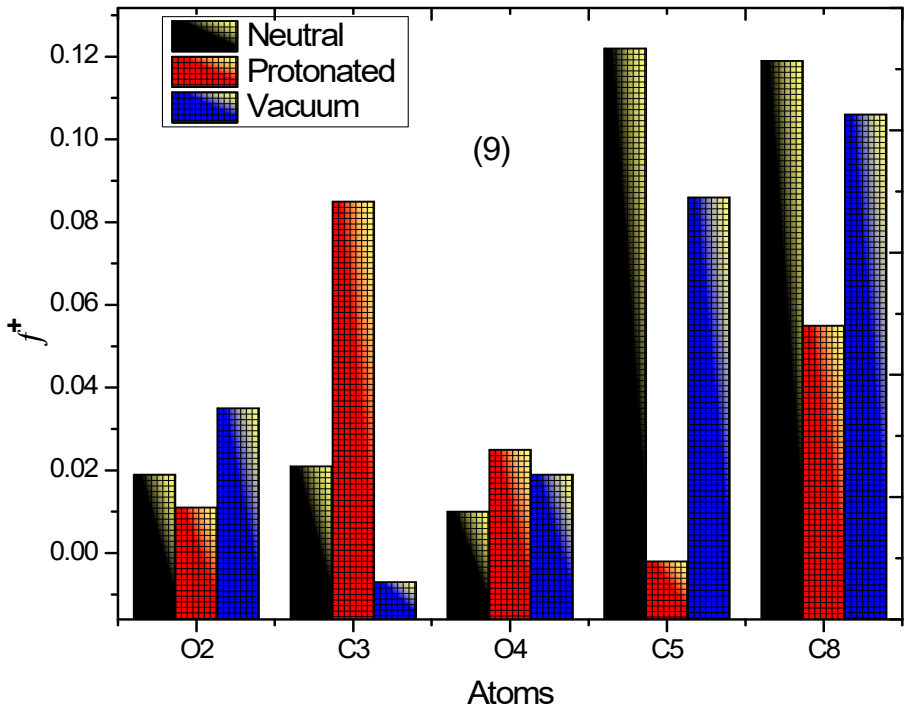
Neutral
Protonated
Vacuum
(9)
0.12
0.10
0.08
0.06
0.04
0.02
0.00
f^+
O2
C3
O4
C5
C8
Atoms

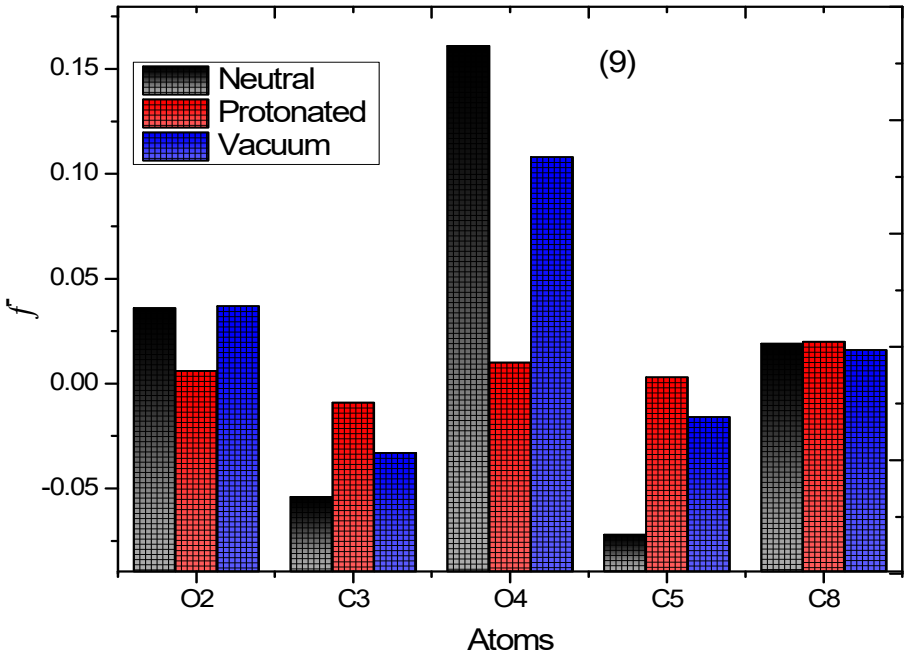
Neutral
Protonated
Vacuum
(9)
0.15
0.10
0.05
0.00
-0.05
f^-
O2
C3
O4
C5
C8
Atoms

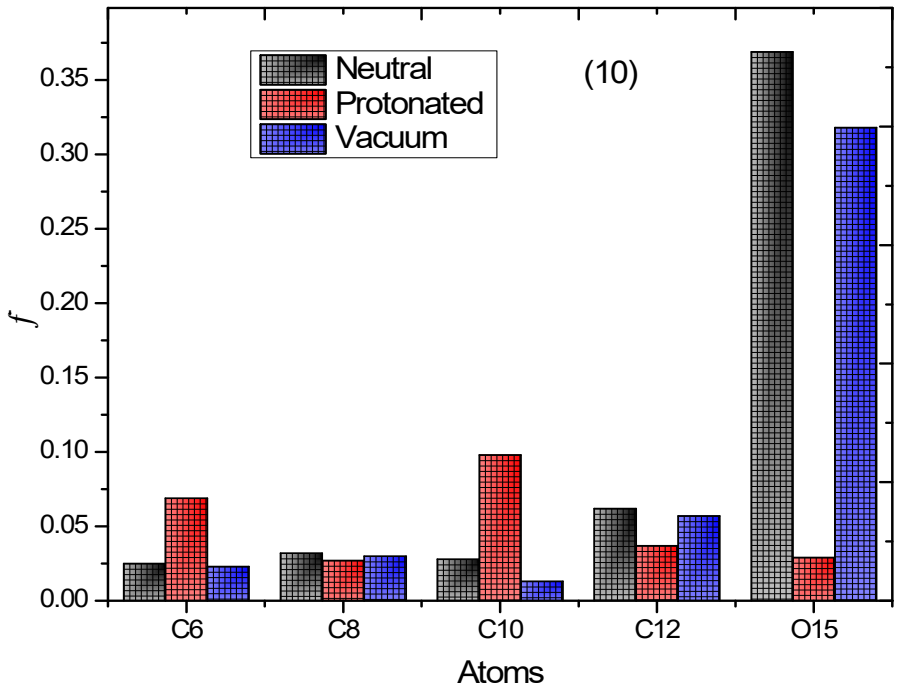
Neutral
Protonated
Vacuum
(10)
0.35
0.30
0.25
0.20
0.15
0.10
0.05
0.00
f
C6
C8
C10
C12
O15
Atoms

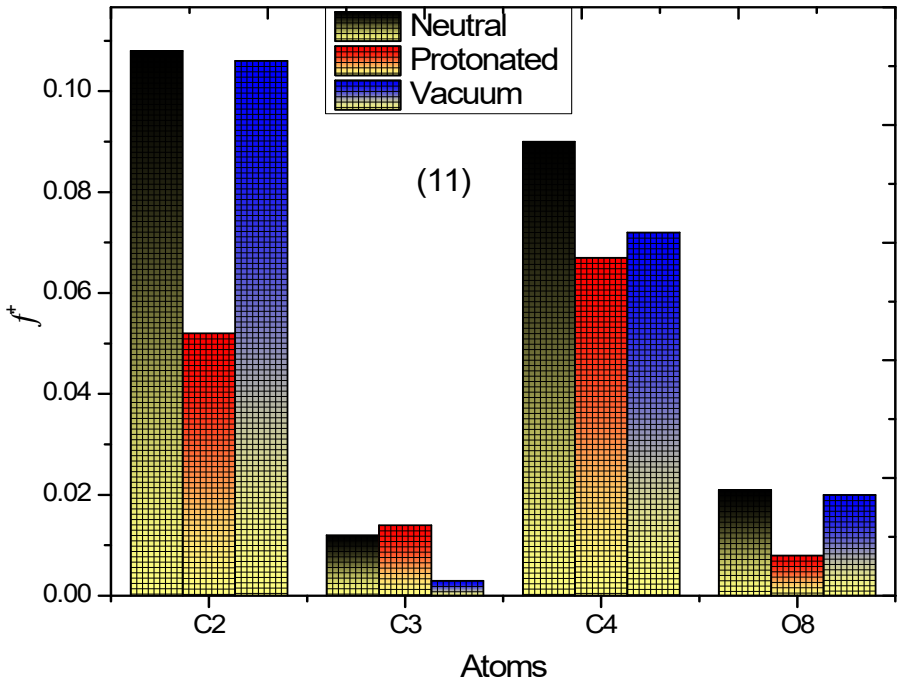
Neutral
Protonated
Vacuum
(11)
0.10
0.08
0.06
0.04
0.02
0.00
f+
C2
C3
C4
O8
Atoms

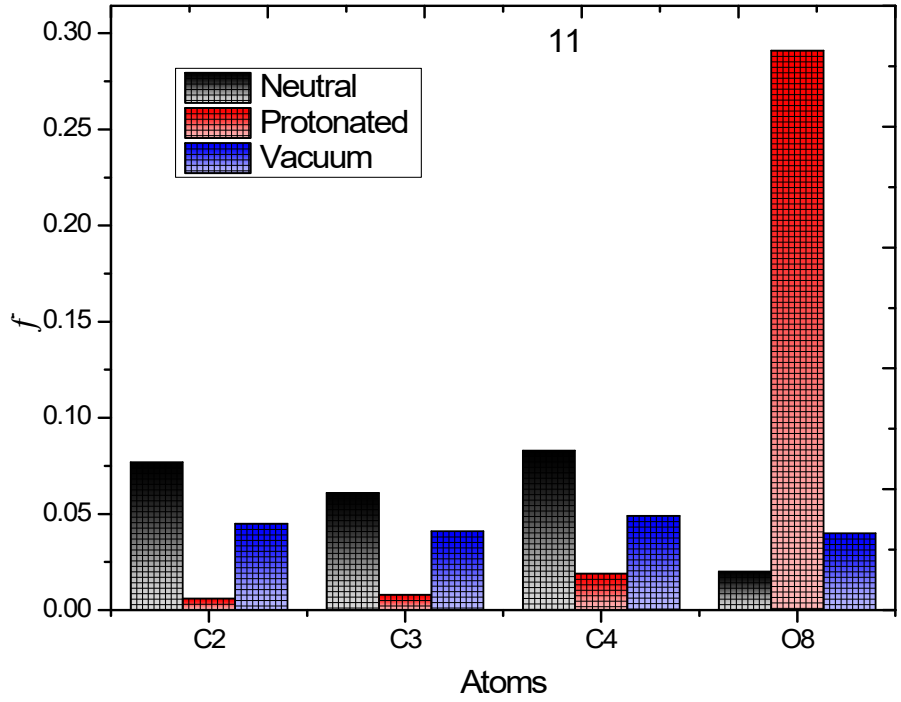
11
Neutral
Protonated
Vacuum
0.30
0.25
0.20
0.15
0.10
0.05
0.00
f-
C2
C3
C4
O8
Atoms

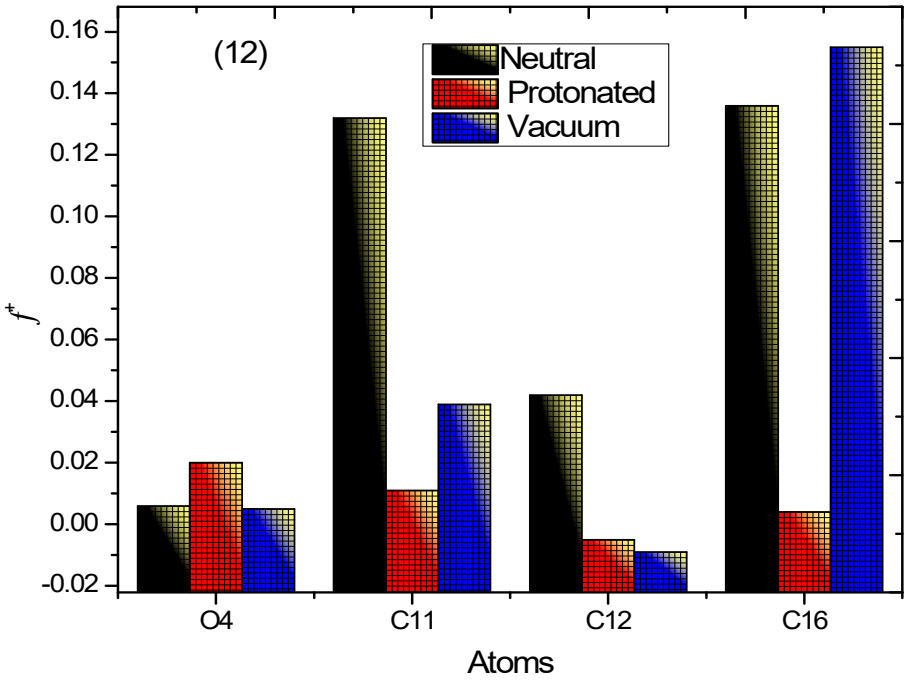
(12)
Neutral
Protonated
Vacuum
0.16
0.14
0.12
0.10
0.08
0.06
0.04
0.02
0.00
-0.02
f+
O4
C11
C12
C16
Atoms

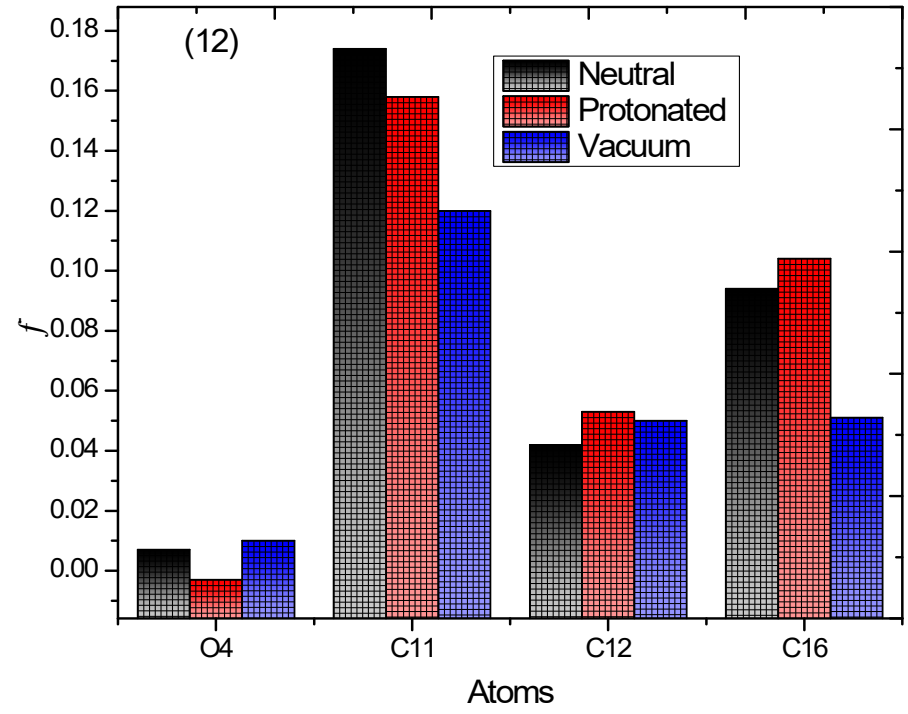
(12)
Neutral
Protonated
Vacuum
0.18
0.16
0.14
0.12
0.10
0.08
0.06
0.04
0.02
0.00
f
O4
C11
C12
C16
Atoms

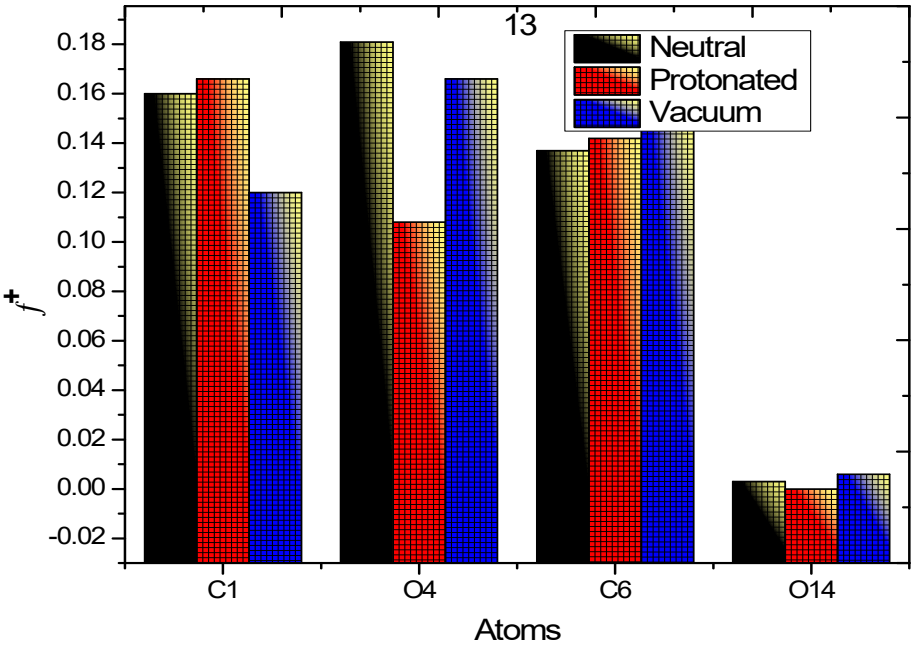

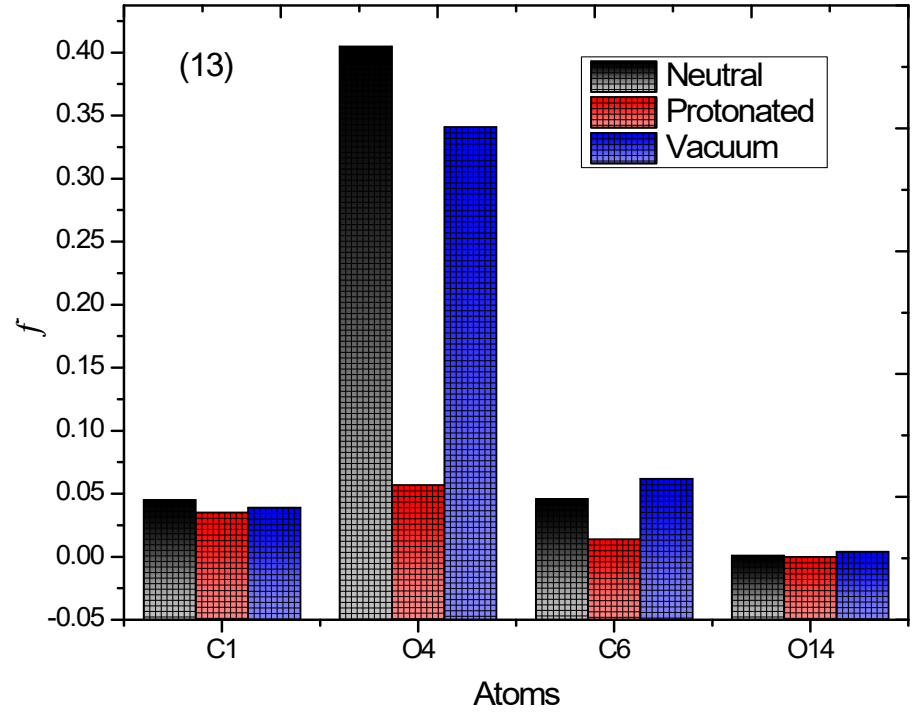

Fig. S11. Atomic structures of the myrrh extract components, highlighting elevated values of Fukui functions (f^{-}_{k} and f^{+}_{k}).